



## Separation of nickel(II) ions from synthetic aqueous solutions with novel dimethylglyoxime-modified Amberlite IRA-420: kinetic and equilibrium studies

Z.A. Khan<sup>a</sup>, A.E.M. Mekky<sup>a,b</sup>, A.S. Bin Mahfouz<sup>c</sup>, T.S. Saleh<sup>a,d</sup>, M.S. Mohy Eldin<sup>a,e,\*</sup>

<sup>a</sup>Chemistry Department, Faculty of Science, University of Jeddah, Asfan P.O. Box 80203, Jeddah 21589, Saudi Arabia, email: ziyakhan@gmail.com (Z.A. Khan)

<sup>b</sup>Chemistry Department, Faculty of Science, Cairo University, Giza, Egypt, email: ataher2211@yahoo.com

<sup>c</sup>Faculty of Engineering, Department of Materials and Chemical Engineering, University of Jeddah, Asfan P.O. Box 80203, Jeddah 21589, Saudi Arabia, Tel. +966 0126952037 Ext. 74255; email: asbinmahfouz@uj.edu.sa

<sup>d</sup>Green Chemistry Department, National Research Centre, Dokki, Cairo 12622, Egypt, email: tamsaid@yahoo.com

<sup>e</sup>Polymer Materials Research Department, Advanced Technology, and New Materials Research Institute, SRTA-City, New Borg El-Arab City 21934, Alexandria, Egypt, Tel. +966 569006640; email: mmohyeldin@srtacity.sci.eg

Received 2 February 2017; Accepted 23 June 2017

### ABSTRACT

In this study, the kinetic and equilibrium results obtained for Ni(II) ions sorption with different initial concentrations onto dimethylglyoxime-modified Amberlite IRA-420 (DMG-AMB) were analyzed. Fast equilibrium was reached after only 10 min where the removal percentage increased from around 60% to 90% with nickel(II) ions concentrations ranged from 3.0 to 15.0 mg/L. On the other hand, the capacity of the adsorbent increased linearly from 0.2 to 1.4 mg/g. The analysis of the kinetic data indicated that the sorption was a second-order process. An ion-exchange mechanism may have existed in the Ni(II) ions sorption process with DMG-AMB. The Ni(II) ions uptake by DMG-AMB quantitatively evaluated with equilibrium sorption isotherms. The maximum sorption capacity, determined from the Dubinin–Radushkevich (D–R) isotherm, was 15.067 mg/g. Moreover, diffusion mechanism of Ni(II) ions was described by different removal–diffusion models. The diffusion rate equations inside particulate of Dumwald–Wagner and intraparticle models were used to calculate the diffusion rate. The actual rate-controlling step involved in the Ni(II) ions sorption process was determined by the further analysis of sorption data by the kinetic expression given by Boyd.

*Keywords:* Metal ions removal; Ni(II) ions; Cation–anion exchanger; Amberlite IRA-420; DMG

### 1. Introduction

Toxic metal ions are found in the industrial effluents and present a real threat for the environment, and their removal is necessary [1,2]. The accumulation in the biological systems and the toxicity manipulates the negative effect of the toxic heavy metals on the aquatic life [3–7]. Nickel is toxic and causes inhibition of oxidative enzyme activity and at high concentrations reduce of nitrogen availability and impaired growth. Above all, it is highly carcinogenic. It is released from

alloys and electroplating industries. Accordingly, it is essential to remove from any effluents before being discharged into aquatic streams. Different classical methods can be used to remove the metal ions from the contaminated industrial effluents [8–10]. Among different materials used for the removal of heavy metals ions, the polymer adsorbents and their composites have shown high capabilities based on their removal and ion-exchange properties [11–17]. Sulfonated polyglycidyl methacrylate has been used in the removal of cadmium ions from aqueous synthetic solutions [18,19].

Amberlite is anions exchanger used for the exchange of anions from wastewater effluents. Metal ions such Mn(VII) and Cr(VI) have been removed previously by Amberlite

\* Corresponding author.

IRA-420 [20–22]. Different polymers have been investigated for the removal of nickel ions. Novel sodium alginate–gelatin blend membranes have been developed [23]. Carbonized sawdust was impregnated with poly(sodium 4-styrene sulfonate) to enhance the nickel(II) affinity and selectivity via surface chelating ion-exchange as well as hydrogen bonding removal mechanism [24]. Removal of nickel ions from aqueous solution by low energy-consuming sorption process involving thermosensitive copolymers with phosphonic acid groups has been investigated [25]. Recently, DMG as a selective ligand for Ni(II) was supported on NCP to prepare a selective sorbent for removal of Ni(II) cations from aqueous solution [26].

In this work, Amberlite IRA-420 anions exchanger has been modified with dimethylglyoxime (DMG) to induce affinity for complexation with Ni(II) ions. The kinetics and the isothermal studies for the removal process have been studied, and the obtained results have been analyzed.

## 2. Materials and methods

### 2.1. Materials

Amberlite (IRA-420) ion-exchange resin was supplied by Rohm and Haas, Philadelphia, USA. It is an amine quaternary cross-linked styrene/divinylbenzene copolymer. Table 1 shows a summary of the resin properties [27].

Sodium hydroxide (NaOH), minimum assay 99%, DMG ( $\text{CH}_3\text{C}(\text{=NOH})\text{C}(\text{=NOH})\text{CH}_3$ ), minimum assay  $\geq 97.0\%$ , and nickel(II) nitrate hexahydrate ( $\text{Ni}(\text{NO}_3)_2 \cdot 6\text{H}_2\text{O}$ ), assay 99.999%, supplied by Sigma-Aldrich, Germany.

### 2.2. Methods

#### 2.2.1. Preparation of dimethylglyoxime-modified Amberlite ions exchanger

Sodium hydroxide solution (0.1 N) was used as a solvent for the preparation of 0.1 N DMG solution. Amberlite IRA-420 (AMB; 10 g) was added to 100 mL of the DMG solution, and the slurry was thermostated at  $60^\circ\text{C}$  under magnetic stirring for 24 h. The DMG-modified Amberlite (DMG-AMB) beads were separated and successively washed with hot water to remove excess of unreacted DMG and NaOH. The polymer beads were kept at room temperature for further use.

Table 1  
Properties of the resin Amberlite IRA-420

Producer	Rohm and Haas
Functionality	$-\text{N}^+(\text{CH}_3)_3$
Matrix type	Polystyrene–divinyl benzene
Standard ionic form	$\text{Cl}^-$
Total exchange capacity (meq/g)	3.80
Bed porosity	0.32
Wet resin density ( $\text{g}/\text{cm}^3$ )	1.15
Bed density ( $\text{g}/\text{cm}^3$ )	0.68
pH operating range	0–14
Maximum operating temperature	$77^\circ\text{C}$
Mean wet particle radius (mm)	0.30–0.70

### 2.2.2. Determination of nickel ions concentration

Conductance measurements were carried out using a conductivity meter supplied by Jenway, UK (model no. 4510). The cell constant was 1.03. The conductivity cell was calibrated with standard KCl solution. The precision of the measurement was within  $0.05 \mu\text{S}/\text{cm}$ . All the solutions are prepared in deionized water whose conductance was within  $1\text{--}2 \mu\text{S}/\text{cm}$ .

A stock solution of Ni(II) was prepared (25 ppm), and from this solution, required concentration of Ni was prepared by dilution with the deionized water. A standard curve for the conductance of different Ni(II) ions concentration was obtained (Fig. 1).

From the slope, we can derive the following relation between conductance and concentration:

$$\text{Concentration (ppm)} = \text{conductance} \times \text{constant (1/slope)} \quad (1)$$

### 2.2.3. Removal experiment

The removal experiments were carried out in a batch process by using nickel aqueous solution. The nickel ions removal studies have been performed by mixing 0.1 g of wet DMG-modified Amberlite IRA-420 with 10 mL of specific nickel concentration. The mixture was agitated at room temperature using magnetic stirrer for 30 min then left to settle for 1 min to separate the adsorbent out of the liquid phase. The nickel ions concentration at ppm, before and after the removal, for each solution, were determined by measuring the conductance and multiplying by 0.7326 constant extracted from the slope of the standard curve. The nickel ions removal percentage was calculated according to the following formula:

$$\text{Nickel ions removal (\%)} = [(C_0 - C_t)/C_0] \times 100 \quad (2)$$

where  $C_0$  and  $C_t$  (mg/L) are the initial at zero time and the final concentration of nickel ions at a specific time, respectively.

The removal capacity is calculated according to the following formula:

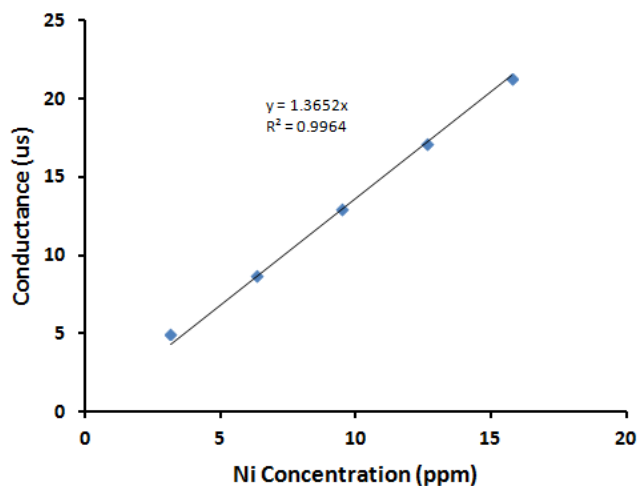


Fig. 1. Standard curve of  $\text{Ni}^{2+}$  ions concentrations.

$$q \text{ (mg/g)} = V (C_0 - C_t) / M \quad (2.1)$$

where  $q$  is the uptake capacity (mg/g);  $V$  is the volume of the nickel(II) ions solution (mL), and  $M$  is the mass of the modified AMB (g).

#### 2.2.4. Fourier transform infrared spectroscopic analysis

The Fourier transform infrared spectroscopic (FTIR) spectra of the Amberlite and DMG-Amberlite have been recorded with an FTIR spectrometer in the spectral range 4,000–500  $\text{cm}^{-1}$ .

### 3. Results and discussion

#### 3.1. Effect of contact time

The effect of variation contact time on Ni(II) ions removal percentage and removal capacity investigated as shown in Figs. 2 and 3. From Fig. 2, it can be seen that the Ni(II) ions removal percentages have been slightly affected by increasing contact time over 10 min. Very fast equilibrium has achieved

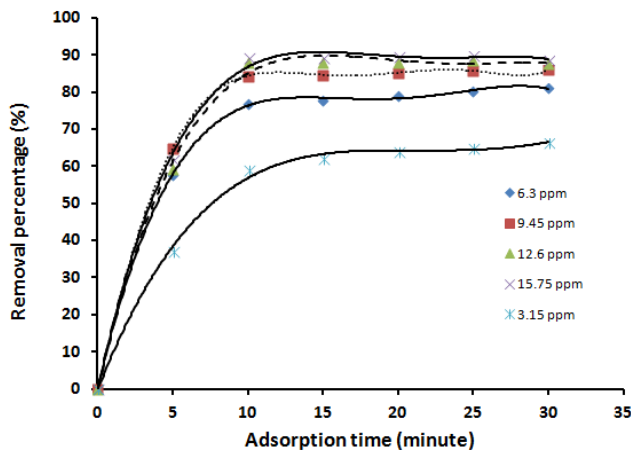


Fig. 2. Effect of adsorption time on Ni<sup>2+</sup> ions removal percentage using DMG-Amberlite ions exchanger.

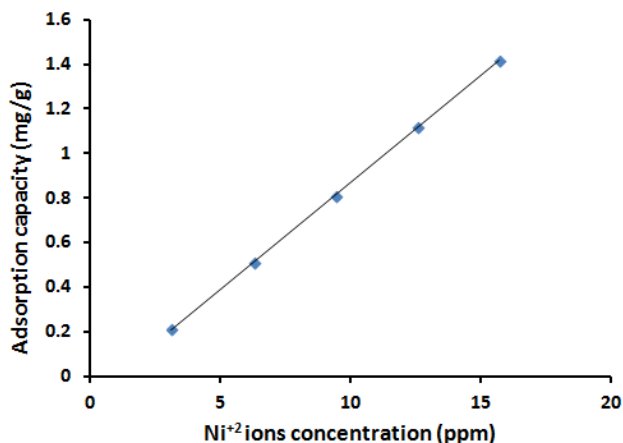


Fig. 3. Effect of Ni<sup>2+</sup> ions concentration on the adsorption capacity of DMG-Amberlite ions exchanger.

due to a high number of available complexation sites. Beyond 10 min removal time, a slight increase of removal percentages was observed. This behavior may refer to the reduction of the concentration gradient between the liquid phase and the adsorbent surface [28]. The similar removal behavior was also observed by Mahmud et al. [29] for the removal of nickel ions from aqueous solution by using polypyrrole conducting polymer and the removal of Co(II) ions from aqueous solution using clinoptilolite nanoparticles modified by glutamic acid (NCP-GLU) [30].

On the other hand, the removal capacity at equilibrium shows a linear increase with the variation of the nickel ions concentration (Fig. 3). This behavior indicates that the capacity of the DMG-AMB beads is not reached the saturation stage yet.

#### 3.2. Sorption kinetic models

Three linear kinetic models were used to describe the kinetics of the sorption process were selected in this study for describing the Ni(II) ions sorption process using DMG-AMB beads.

The pseudo-first-order kinetic model given by Lagergren and Svenska [31]:

$$\ln(q_e - q_t) = \ln q_e - k_1 t \quad (3)$$

The pseudo-second-order rate (chemisorptions) expressed as [32]:

$$t/q_t = (1/k_2 q_e^2) + t/q_e \quad (4)$$

The simple Elovich model represented in the simple form [33]:

$$q_t = \alpha + \beta \ln t \quad (5)$$

where  $q_e$  and  $q_t$  are the amounts of ions adsorbed (mg/g) at equilibrium and time  $t$  (min), respectively.  $k_1$  ( $\text{min}^{-1}$ ) is the first-order reaction rate constant.  $k_2$  is the second-order reaction rate equilibrium constant ( $\text{g/mg min}$ ).  $\alpha$  represents the initial sorption rate ( $\text{mg/g min}$ ), and  $\beta$  is related to the extent of surface coverage and activation energy for chemisorption ( $\text{g/mg}$ ).

The values of the first-order rate constant  $k_1$  and correlation coefficient,  $R^2$  obtained from the slope of the plot  $\ln(q_e - q_t)$  vs. time (Fig. 4) are reported in Table 2. From the table, it was indicated that the correlation coefficients are not high for the different Ni(II) ions concentrations. Also, the estimated values of  $q_e$  calculated from the equation differed from the experimental values, which show that the model is not appropriate to describe the sorption process.

The pseudo-second-order kinetics applies to the experimental data in Fig. 5. From the figure the values of  $q_e$  calculated, and  $k_2$  can be determined from the slope and intercept of the plot, respectively. Also, the values of the correlation coefficients,  $R^2$  for the sorption of different initial concentrations of Ni(II) ions on DMG-AMB beads were tabulated in Table 3. Based on linear regression values from this table ( $R^2 \approx 1$ ), the kinetics of Ni(II) ions sorption on to

DMG-AMB beads can be described well by the second-order equation. Hence, it suggests that the rate-limiting step in these sorption processes may be chemisorptions involving effective forces through the sharing or exchanging of electrons between sorbent and sorbate [34]. Additionally, comparing the values of  $q_e$  (calculated) resulted from the intersection points of the second-degree reaction kinetic curves (Table 3) with that obtained from the experimental data for the different studied Ni(II) ions

concentrations. Thus, second-order rate expression fits the data most satisfactorily.

From Fig. 6, the estimated Elovich equation parameters were tabulated in Table 4. The value of  $\beta$  is indicative of the number of sites available for removal while  $\alpha$  is the removal quantity when  $\ln t$  is equal to zero; that is, the removal quantity when  $t$  is 1 h (equilibrium time). This value is giving insight about the removal behavior of the first step [35]. However, the obtained data according to the Elovich equation does not fit well with the experimental data.

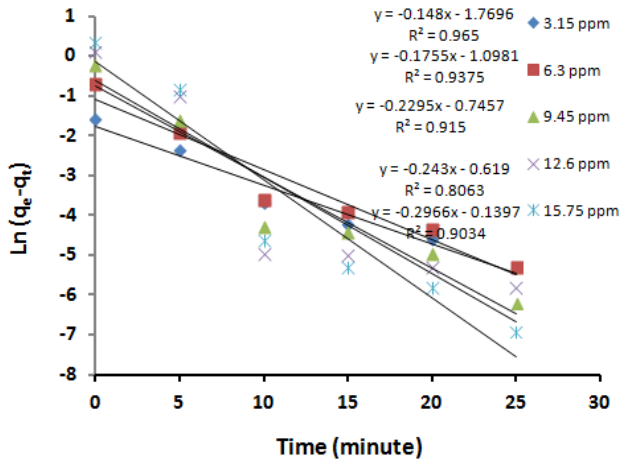


Fig. 4. First-order plots for different Ni<sup>2+</sup> ions concentration removal using DMG-Amberlite ions exchanger.

Table 2  
Estimated kinetic parameter of the first-order rate model and comparison between the experimental and calculated  $q_e$  values for different Ni<sup>2+</sup> ions concentrations

$C_0$ (mg/L)	$k_1$ (min <sup>-1</sup> )	$q_{exp}$ (mg/g)	$q_{cal}$ (mg/g)	$R^2$
3.15	0.148	0.21	0.17	0.965
6.3	0.1755	0.51	0.333	0.9375
9.45	0.2295	0.812	0.474	0.915
12.6	0.243	1.118	0.538	0.8063
15.75	0.2966	1.415	0.87	0.9034

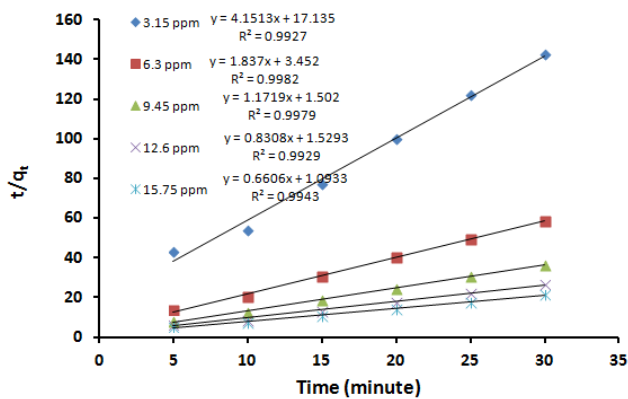


Fig. 5. Second-order plots for different Ni<sup>2+</sup> ions concentration removal using DMG-Amberlite ions exchanger.

### 3.3. Sorption mechanisms

Further models are required to describe the diffusion mechanism. The ideal liquid/solid removal process is described by film diffusion, intraparticle diffusion, and mass action. Since the mass action is a very rapid process,

Table 3  
Estimated kinetic parameters of the second-order rate model and comparison between the experimental and calculated  $q_e$  values for different Ni<sup>2+</sup> ions concentrations

$C_0$ (mg/L)	$k_2$ (g/mg min)	$q_{exp}$ (mg/g)	$q_{cal}$ (mg/g)	$R^2$
3.15	17.135	0.21	0.241	0.9927
6.3	3.452	0.51	0.544	0.9982
9.45	1.502	0.812	0.835	0.9979
12.6	1.5293	1.118	1.20	0.9929
15.75	1.0933	1.415	1.51	0.9943

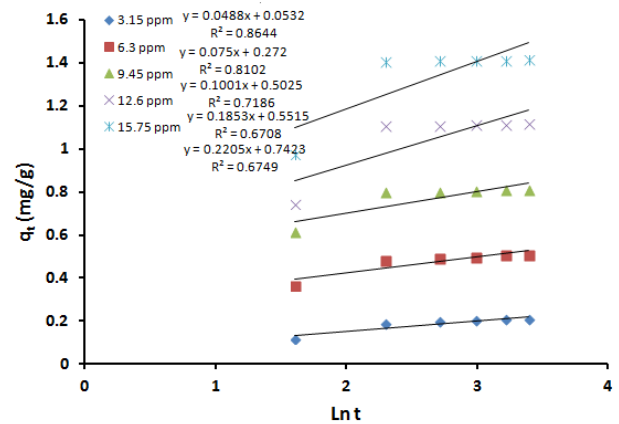


Fig. 6. Simple Elovich plots for different Ni<sup>2+</sup> ions concentration removal using DMG-Amberlite ions exchanger.

Table 4  
Parameters obtained from the simple Elovich model for different Ni<sup>2+</sup> ions concentration

$C_0$	$\alpha$ (mg/g min)	$\beta$ (g/mg)	$R^2$
3.15	0.0523	0.0488	0.8644
6.3	0.272	0.075	0.8102
9.45	0.5025	0.1001	0.7186
12.6	0.5519	0.1848	0.6713
15.75	0.7423	0.2205	0.6749

so the rate-limiting step is the liquid film diffusion or intraparticle diffusion [36,37]. The diffusion rate equations inside particulate of Dumwald–Wagner and intraparticle models were used to calculate the diffusion rate of Ni(II) ions through DMG-AMB beads. On the other hand concerning the external mass transfer, Boyd model was examined to determine the actual rate-controlling step for the Ni(II) ions removal.

The diffusion rate equation inside particulate of Dumwald–Wagner can be expressed as [38]:

$$\log(1 - F^2) = -(K/2.303) \times t \tag{6}$$

where  $K$  is the diffusion rate constant and the removal percentage,  $F$  is calculated by  $(q_t/q_e)$ . The linear plots of  $\log(1 - F^2)$  vs.  $t$  (Fig. 7) indicate the applicability of this kinetic model. The diffusion rate constants for Ni(II) ions diffusion inside DMG-AMB beads are tabulated in Table 5.

The intraparticle model commonly is used for identifying the removal mechanism. The intraparticle equation is written as follows [39]:

$$q_t = k_d t^{1/2} + C \tag{7}$$

The intraparticle diffusion plot for Ni(II) ions removal onto DMG-AMB is given in Fig. 8. Two separate linear portions that represent each line could observe from the figure. These two linear portions in the intraparticle model suggest

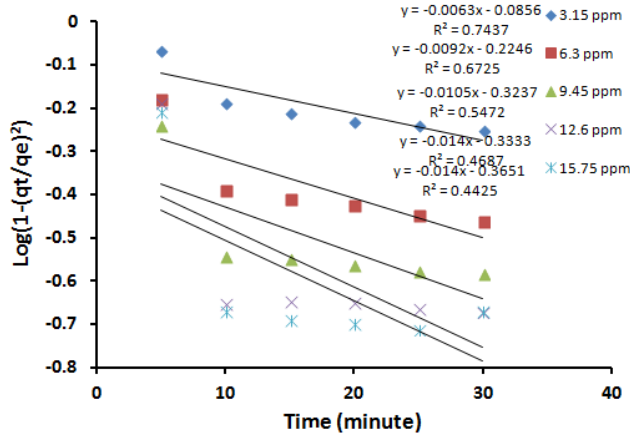


Fig. 7. Dumwald–Wagner plots for intraparticle diffusion using different Ni<sup>2+</sup> ions concentration removal using DMG-Amberlite ions exchanger.

Table 5  
Parameters obtained from Dumwald–Wagner diffusion model for different Ni<sup>2+</sup> ions concentrations

C <sub>0</sub> (mg/L)	K (min <sup>-1</sup> )	R <sub>1</sub> <sup>2</sup>
3.15	0.0145	0.7437
6.3	0.0211	0.6725
9.45	0.0242	0.5472
12.6	0.0322	0.4687
15.75	0.322	0.4425

that the removal process consists of both surface removal and intraparticle diffusion. While the initial linear portion of the plot is the indicator of boundary layer effect, the second linear portion is due to intraparticle diffusion [40]. The intraparticle diffusion rate ( $k_d$ ) calculated from the slope of the second linear portion and given in Table 6. The value of  $C$  provides an idea about the thickness of the boundary layer (Table 6).

The larger the intercept, the greater is the boundary layer effect [41]. Increasing of initial Ni(II) ions concentration leads to the increase in boundary layer effect for Ni(II) ions removal, which by its rule decreased the intraparticle diffusion rate as discussed.

The sorption data were further analyzed by the kinetic expression is given by Boyd et al. [42] to characterize what the actual rate-controlling step involved in the Ni(II) ions sorption process.

$$F = 1 - (6/\pi^2) \exp(-B_t) \tag{8}$$

where  $F$  is the fraction of solute sorbed at different time  $t$  and  $B_t$  is a mathematical function of  $F$  and given by the following equation:

$$F = q/q_\infty \tag{9}$$

where  $q$  and  $q_\infty$  represent the amount sorbed (mg/g) at any time  $t$  and at infinite time (in the present study 30 min).

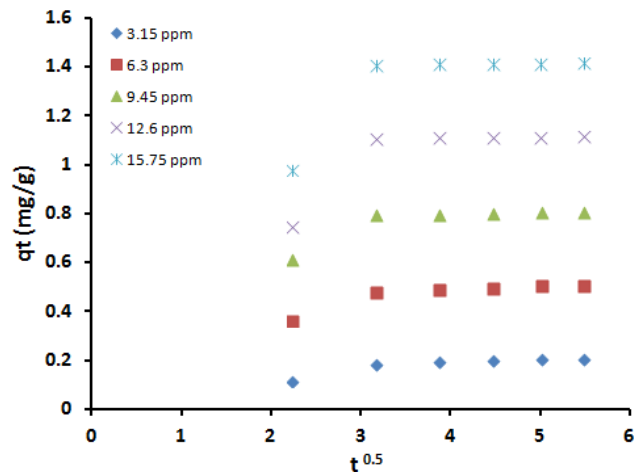


Fig. 8. Intraparticle diffusion plots for different Ni<sup>2+</sup> ions concentration removal using DMG-Amberlite ions exchanger.

Table 6  
Parameters obtained from the intraparticle diffusion model for different Ni<sup>2+</sup> ions concentrations

C <sub>0</sub> (ppm)	k <sub>d</sub> (mg/(g min <sup>1/2</sup> ))	C	R <sup>2</sup>
3.15	0.0105	0.153	0.9901
6.3	0.0119	0.4446	0.9948
9.45	0.0065	0.7763	0.9665
12.6	0.0029	1.1013	0.9363
15.75	0.0042	1.3926	0.9537

With substituting Eq. (8) into Eq. (9), the kinetic expression becomes:

$$B_t = -0.4978 - \ln(1 - q/q_\infty) \quad (10)$$

Thus, the value of  $B_t$  can calculate for each value of “F” using Eq. (10). The calculated  $B_t$  values were plotted against time as shown in Fig. 9. The linearity of this plot will provide useful information to distinguish between external transport and intraparticle transport controlled rates of sorption. Fig. 9 shows the plot of  $B_t$  vs.  $t$  for different initial Ni(II) ions concentrations, which were straight lines that do not pass through the origin, indicating that film diffusion governs the rate limiting process [43]. The methyl hydrophobic groups of DMG play a significant role in changing the hydrophilic–hydrophobic balance of the Amberlite beads and accordingly, in a way or another, the thickness of the formed liquid boundary layer over the solid surface and leads to make the film diffusion is the limiting process [44].

### 3.4. Sorption isotherm models

The most common isotherm models used in almost all the publications deal with the characterization of adsorption process are Freundlich and Langmuir isotherm models. The two models are opposite to each other.

The Freundlich isotherm is a widely used equilibrium isotherm model but provides no information on the monolayer sorption capacity, in contrast to the Langmuir model [45,46]. The Freundlich isotherm model is the first used isotherm model which postulates heterogeneous surfaces site energies and multilayers levels of sorption. The mathematical linear formula of the model is expressed as the following equation [47]:

$$\ln q_e = \ln K_f + 1/n_f \ln C_e \quad (11)$$

where  $q_e$  (mg/g) and  $C_e$  (mg/L) represent the adsorbent capacity and the adsorbate ions concentration at equilibrium. The indicators of the adsorption capacity and adsorption intensity are given by  $K_f$  and  $n_f$  Freundlich constants.

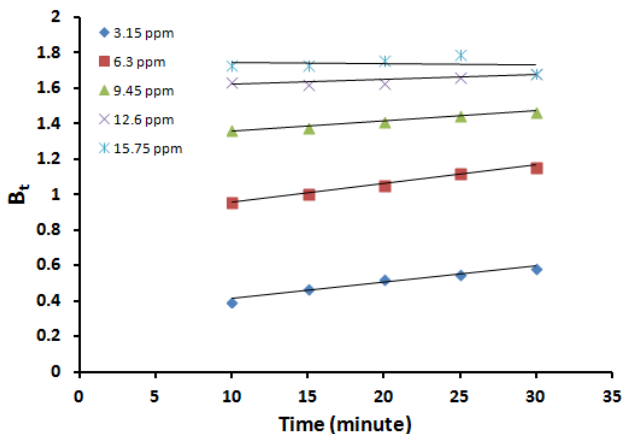


Fig. 9. Boyd expression of the sorption of different Ni<sup>2+</sup> ions concentrations using DMG-Amberlite ions exchanger.

Linear fits of the sorption data of Ni(II) ions were provided in Fig. 10. According to the figure, the Freundlich equation predicts that the Ni(II) ions concentration on the sorbents will increase as long as there is an increase in the Ni(II) ions concentration; this is compatible with the experimental results. Furthermore, by the correlation coefficient ( $R^2$ ) value (0.9487), it was demonstrated that the removal of Ni(II) ions obeyed the Freundlich isotherm. The values of Freundlich constants  $n_f$  (0.2143) and  $K_f$  (0.1917) are estimated from the slope and intercept of the linear plot. From the assessed value of  $n_f$ , it was found that  $n_f < 1$  dictated non-favorable sorption for Ni(II) ions with the DMG-AMB beads [48].

On the other hand, the Langmuir isotherm assumes completely homogeneous surface with a finite number of identical sites and with a negligible interaction between adsorbed molecules which results in monolayer sorption. The linear mathematical formula of the model is presented by the following equation [49]:

$$C_e/q_e = 1/q_m K + C_e/q_m \quad (12)$$

where  $q_m$  is the maximum monolayer adsorption capacity (mg/g), and  $K$  is the adsorption energy (L/mg).

A plot of  $C_e/q_e$  vs.  $C_e$  should present a straight line of slope  $1/q_m$  and intercept  $1/q_m K$ . Fig. 11 illustrates a linear plot of the Langmuir equation for Ni(II) ions removal with the DMG-AMB polymers at various initial Ni(II) ions concentrations. According to the  $R^2$  value, the Langmuir equation represents the sorption process of Ni(II) ions not very well; the  $R^2$  value is 0.7545. That indicates a bad mathematical fit. It was found from the calculated values of  $q_m$  is 0.1473 mg/g and of  $K$  is 1.66 L/mg. That indicates that the DMG-AMB was highly efficient for Ni(II) ions removal and had a low energy of sorption (1.66 L/mg) which referred to the affinity of DMG toward the Ni(II) ions.

To predict the favorable or unfavorable of the adsorption system, essential characteristics defined by a dimensionless

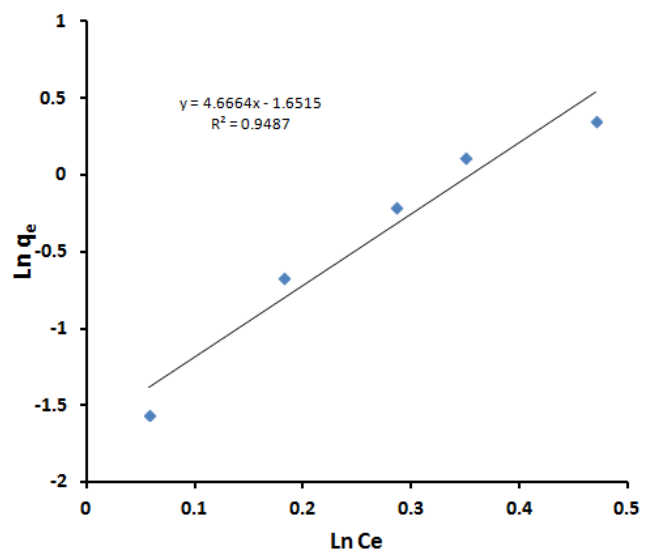


Fig. 10. Freundlich isotherm for Ni<sup>2+</sup> ions removal with various initial solution concentrations using DMG-Amberlite ions exchanger.

separation factor ( $R_L$ ) used and calculated according to the following equation [50]:

$$R_L = 1/(1 + KC_0) \tag{13}$$

where  $C_0$  is the Ni(II) ions initial concentration (mg/L). The calculated values of  $R_L$  for Ni(II) ions removal (Table 7) show favorable removal because the  $R_L$  values fall between 0 and 1 [51,52]. That again confirms that the Langmuir isotherm was favorable for the sorption of Ni(II) ions onto DMG-AMB under the conditions used in this study. This result is in agreement with previously published results of the removal of Ni(II) ions using modified Iranian natural clinoptilolite with DMG [26]. They claimed that monolayer's adsorption also confirms a chemisorption occurs for Ni(II) removal via a complexation between Ni(II) and DMG on NCP-DMG sorbent

Other isotherm models comprise between the Freundlich and Langmuir isotherm models such as the D–R isotherm and the Temkin isotherm. The D–R isotherm is a derivative from the Langmuir isotherm but more general where rejects the constant adsorption potential assumption [48]. The D–R isotherm expressed as follows:

$$\ln q_e = \ln V'_m - K'\epsilon^2 \tag{14}$$

where  $q_e$  is the amount of Ni(II) ions removed per unit of adsorbent mass (mg/g),  $V'_m$  is the D–R sorption capacity (mg/g),

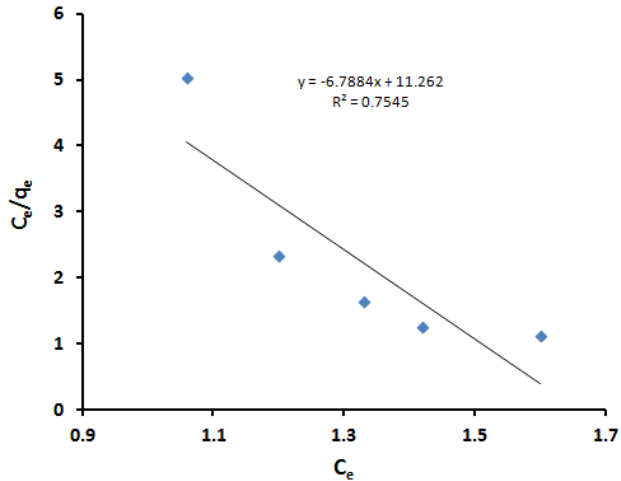


Fig. 11. Langmuir isotherm for Ni<sup>2+</sup> ions removal with various initial solution concentrations using DMG-Amberlite ions exchanger.

Table 7  
The  $R_L$  values for different initial Ni<sup>2+</sup> ions concentrations

$C_0$ (mg/L)	$R_L$
3.15	0.36
6.3	0.33
9.45	0.31
12.6	0.3
15.75	0.27

$K'$  is a constant related to the removal energy ( $\text{mol}^2/\text{k}^2$ ), and  $\epsilon$  is the Polanyi potential.  $\epsilon$  calculated with the following equation:

$$\epsilon = RT(1 + 1/C_e) \tag{15}$$

where  $R$  is the gas constant ( $8.314 \times 10^{-3} \text{ kJ/mol K}$ ), and  $T$  is the temperature (K). The constant  $K'$  gives the mean free energy of sorption per molecule of the sorbate ( $E$ ) when it is transferred to the surface of the solid from infinity in the solution.

This energy gives information about the physical and chemical features of the sorption process [52] and can compute with the following relationship [53]:

$$E = (2K')^{-0.5} \tag{16}$$

This energy gave information about the sorption mechanism and perceived as the amount of energy required to transfer 1 mol of the adsorbate from infinity in the bulk of the solution to the site of sorption. If  $E$  is between 8 and 20 kJ/mol, the sorption process follows chemical ion-exchange, and if  $E > 8 \text{ kJ/mol}$ , the sorption process has a physical nature [54,55].

The D–R isotherm model applied to the equilibrium data obtained from the empirical studies for Ni(II) ions removal using DMG-AMB to determine the nature of the sorption processes (physical or chemical). A plot of  $\ln q_e$  against  $\epsilon^2$  is given in Fig. 12. The D–R plot yields a straight line with the  $R^2$  value equal to 0.9797, and this indicates that the D–R model fits well with the experimental data in comparison with the Langmuir and Freundlich isotherm models. According to the plotted D–R isotherm, the model parameters  $V'_m$ ,  $K'$ , and  $E$  are determined, and their values are 15.076 mg/g, 1.5438  $\text{mol}^2/\text{k}^2$ , and 0.57 kJ/mol, respectively. The calculated removal energy ( $E < 8 \text{ kJ/mol}$ ) indicates that the nickel ions sorption processes could be considered physisorption in nature [56]. Therefore, it is possible that physical means such as electrostatic forces played a significant role as sorption mechanisms for the sorption of nickel ions in this work. The adsorption of other metal ions onto different

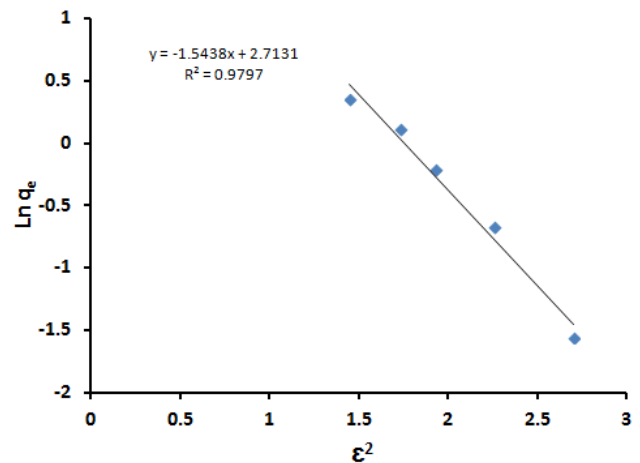


Fig. 12. D–R isotherm for Ni<sup>2+</sup> ions removal with various initial solution concentrations using DMG-Amberlite ions exchanger.

adsorbents has been founded fitted with D–R isotherm. For example, natural clinoptilolite tuff modified with hexadecyltrimethylammonium bromide and dithizone in the removal of Pb(II) cations [57] and aspartic acid modified clinoptilolite in the removal of Cu(II) ions [58].

Finally, the Temkin isotherm taking into account the impact of indirect adsorbent/adsorbate interactions on the adsorption process which reduced in a linear way the heat of adsorption of all molecules in a layer [59]. That can be expressed in a linear form as follows [60]:

$$q_e = B \ln K_T + B \ln C_e \quad (17)$$

where  $K_T$  is the Temkin equilibrium binding constant corresponding to the maximum binding energy, and  $B$  is the Temkin constant related to the heat of sorption. A plot of  $q_e$  vs.  $\ln C_e$  (Fig. 13) enables the determination of isotherm constants  $B$  and  $K_T$  from the slope and the intercept, respectively.

The calculated value of  $K_T$  is 1 L/g, and this represents the equilibrium binding constant corresponding to the maximum binding energy; however, constant  $B$ , which is 3.0173 J/mol, is related to the heat of sorption for DMG-AMB matrix.

Finally, all the  $R^2$  values obtained from the four equilibrium isotherm models applied to nickel ions sorption on DMG-AMB beads are summarized. The Temkin isotherm model yielded the highest  $R^2$  value (0.9902), and this showed that nickel ions sorption on the polymer described well by this model which considers the effects of indirect adsorbent/adsorbate interactions on the removal process. The heat of removal of all molecules in a layer decreases linearly with coverage because of adsorbent/adsorbate interactions. On the other hand, the D–R model yielded the next highest  $R^2$  value (0.9797). That suggested that it was possible that electrostatic forces played a significant role as sorption mechanisms for the sorption of nickel ions by DMG-AMB matrix.

### 3.5. FTIR analysis

The characteristic bands for the AMB polymeric backbone, poly(styrene-*co*-divinylbenzene), have been shown in the spectrum at 700, 800, 900, 1,000, 1,400–1,600, and

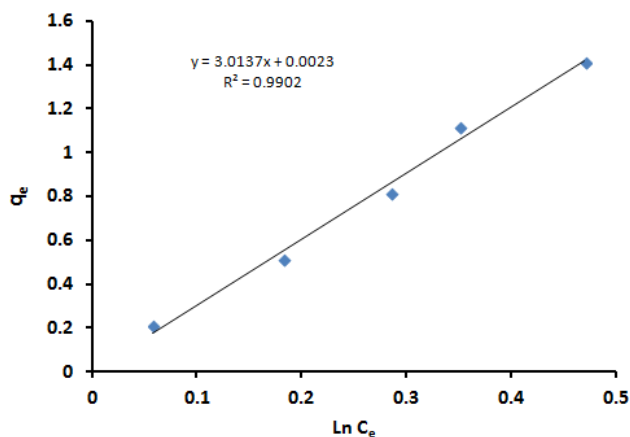


Fig. 13. Temkin isotherm for Ni<sup>2+</sup> ions removal with various initial solution concentrations using DMG-Amberlite ions exchanger.

2,900–3,000 cm<sup>-1</sup> [61]. The characteristic band for DMG recognized at DMG-AMB shows the peaks at 467 and 904 cm<sup>-1</sup> which relate to the skeleton deformation vibration of DMG molecules. The peaks at 707 and 980 cm<sup>-1</sup> are attributed to the (CNO) bending vibration and (NO) stretching vibration modes, respectively. The symmetrical and asymmetrical deformation vibrations of (CH<sub>3</sub>) appear at 1,364 and 1,444 cm<sup>-1</sup>, respectively. The weak peak at 2,930 cm<sup>-1</sup> is due to the (CH<sub>3</sub>) symmetrical stretching vibration (Fig. 14). The relative broad peak at 3,207 cm<sup>-1</sup> is attributed to the (OH) stretching vibration. But its lower intensity in comparison with that of the free (OH) group is due to the intramolecular hydrogen bonding which will be favored for the structural pattern of the DMG molecule itself [26].

## 4. Conclusion

Novel DMG-modified Amberlite IRA-420 (DMG-AMB) cations exchanger has been prepared and used for the separation of Ni(II) ions. The treatment of Amberlite with DMG has been succeeded in the conversion of the Amberlite IRA-420 from being an anions exchanger to be a cations exchanger. The DMG-AMB has been successfully removed Ni(II) ions from synthetic solution. The Langmuir parameter for Ni(II) ions removal ( $K$ ) indicates that the DMG-AMB was highly efficient for Ni(II) ions removal and had a low energy of sorption (1.66 L/mg). The essential characteristic of the Langmuir isotherm ( $R_L$ ) shows favorable removal because the  $R_L$  values fall between 0 and 1. The monolayer's adsorption also confirms a chemisorption occurs for Ni(II) removal via a complexation between Ni(II) and DMG on NCP-DMG sorbent. According to Dubinin–Radushkevich (D–R) isotherm, the maximum sorption capacity was found to be 15.067 mg/g. The kinetic data indicated that the sorption was a second-order process. Moreover, diffusion mechanism of Ni(II) ions was described by different removal–diffusion models. The obtained results indicate that the film diffusion is the rate-limiting process.

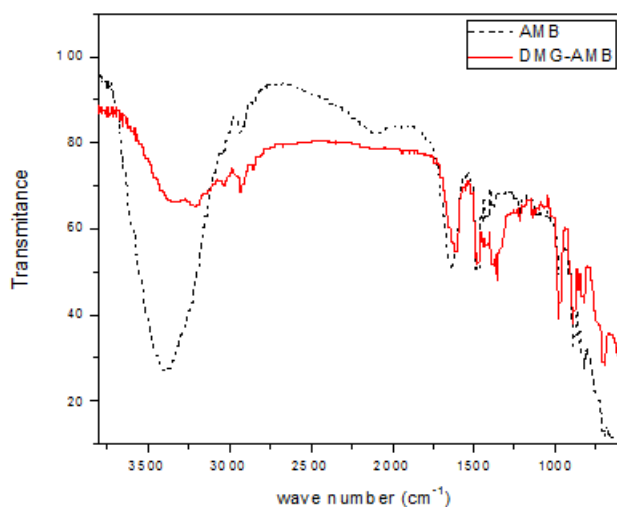


Fig. 14. FTIR spectrum of Amberlite (AMB) and dimethylglyoxime-modified Amberlite (DMG-AMB).

## References

- [1] B.R. Stern, Essentiality and toxicity in copper health risk assessment: overview, update and regulatory considerations, *J. Toxicol. Environ. Health Part A*, 73 (2010) 114–127.
- [2] K.W. Greve, K.J. Bianchini, M.T. Heinly, J.M. Love, D.A. Swift, M. Ciota, Classification accuracy of the Portland digit recognition test in persons claiming exposure to environmental and industrial toxins, *Arch. Clin. Neuropsychol.*, 23 (2008) 341–350.
- [3] N. Sivagangi Reddy, K. Madhusudana Rao, T.J. Sudha Vani, K.S.V. Krishna Rao, Y.I. Lee, Pectin/poly(acrylamide-co-acrylamidoglycolic acid) pH sensitive semi-IPN hydrogels: selective removal of Cu<sup>2+</sup> and Ni<sup>2+</sup>, modeling, and kinetic studies, *Desal. Wat. Treat.*, 57 (2015) 6503–6514.
- [4] K.H. Chu, Removal of copper from aqueous solution by chitosan in prawn shell: removal equilibrium and kinetics, *J. Hazard. Mater.*, 90 (2002) 77–95.
- [5] L. Rogerio, F.V. Tadeu, Competitive removal of Cu(II) and Cd(II) ions by chitosan crosslinked with epichlorohydrin-triphosphate, *Bioresour. Technol.*, 102 (2011) 8769–8776.
- [6] Y.K. Bayhan, B. Keskinler, A. Cakici, M. Levent, Removal of divalent heavy metal mixtures from water by *Saccharomyces cerevisiae* using crossflow microfiltration, *Water Res.*, 35 (2001) 2191–2200.
- [7] A. Karagunduz, D. Unal, New method for evaluation of heavy metal binding to alginate beads using pH and conductivity data, *Adsorption*, 12 (2006) 175–184.
- [8] B. Volesky, Biosorption process simulation tools, *Hydrometallurgy*, 71 (2003) 179–190.
- [9] U. Farooq, J.A. Kozinski, M.A. Khan, M. Athar, Biosorption of heavy metal ions using wheat based biosorbents—a review of the recent literature, *Bioresour. Technol.*, 101 (2010) 5043–5053.
- [10] L. Singh, R.P. Asalapuram, L. Ramnath, K.R. Gunaratna, Effective removal of Cu<sup>2+</sup> ions from aqueous medium using alginate as biosorbent, *Ecol. Eng.*, 38 (2012) 119–124.
- [11] R. Ansari, N.K. Fahim, Application of polypyrrole coated on wood sawdust for removal of Cr(VI) ion from aqueous solutions, *React. Funct. Polym.*, 67 (2007) 367–374.
- [12] H. Eisazadeh, Removal of chromium from waste water using polyaniline, *J. Appl. Polym. Sci.*, 104 (2007) 1964–1967.
- [13] H. Eisazadeh, Removal of arsenic in water using polypyrrole and its composites, *World Appl. Sci. J.*, 3 (2008) 10–13.
- [14] C.W. Lim, K. Song, S.H. Kim, Synthesis of PPy/silica nanocomposites with cratered surfaces and their application in heavy metal extraction, *J. Ind. Eng. Chem.*, 18 (2012) 24–28.
- [15] J. Wang, B. Deng, H. Chen, X. Wang, J. Zheng, Removal of aqueous Hg(II) by polyaniline: sorption characteristics and mechanisms, *Environ. Sci. Technol.*, 43 (2009) 5223–5228.
- [16] Y. Zhang, Q. Li, L. Sun, R. Tang, J. Zhai, High efficient removal of mercury from aqueous 415 solution by polyaniline/humic acid nanocomposite, *J. Hazard. Mater.*, 175 (2010) 404–409.
- [17] M. Omraei, H. Esfandian, R. Katal, M. Ghorbani, Study of the removal of Zn(II) from aqueous solution using polypyrrole nanocomposite, *Desalination*, 271 (2011) 248–256.
- [18] M.S. Mohy Eldin, M.F. Elkady, M.A. Abu-Saied, A.M. Abdel Rahman, E.A. Soliman, A.A. Elzatahry, M.E. Youssef, Removal of cadmium ions from synthetic aqueous solutions using a novel nano-sulphonated poly(glycidylmethacrylate) cation exchanger: kinetic and equilibrium studies, *J. Appl. Polym. Sci.*, 118 (2010) 3111–3122.
- [19] M.S. Mohy Eldin, M.F. Elkady, M.A. Abu-Saied, A.M. Abdel Rahman, E.A. Soliman, A.A. Elzatahry, M.E. Youssef, Novel nano-sulphonated polyglycidyl methacrylate cation exchanger for removal of heavy metals: optimization of the operational conditions, *Desalination*, 279 (2011) 152–162.
- [20] M.S. Mohy Eldin, K. Aly, Z.A. Khan, A.E. Meky, T.S. Saleh, A.S. Elbogamy, Development of novel acid–base ions exchanger for basic dye removal: phosphoric acid doped pyrazole-g-polyglycidyl methacrylate, *Desal. Wat. Treat.*, 57 (2016) 24047–24055.
- [21] M.S. Mohy Eldin, K.M. Aly, Z.A. Khan, A.E.M. Mekky, T.S. Saleh, A.S. Al-Bogami, Removal of methylene blue from synthetic aqueous solutions with novel phosphoric acid-doped pyrazole-g-poly(glycidyl methacrylate) particles: kinetic and equilibrium studies, *Desal. Wat. Treat.*, 57 (2016) 27243–27258.
- [22] M.S. Mohy Eldin, K.A. Alamry, M.A. Al-Malki, Kinetic and isothermal studies of manganese (VII) ions removal using Amberlite IRA-420 anion exchanger, *Desal. Wat. Treat.*, 72 (2017) 30–40.
- [23] T.J.S. Vani, N.S. Reddy, K.S.V.K. Rao, S.R. Popuri, Development of novel blend membranes based on carbohydrate polymers for the removal of toxic metal ions through sorption, *Desal. Wat. Treat.*, 57 (2016) 25729–25738.
- [24] K.M. Tajun Meera Begum, N.M.I. Alhaji, A. Ayeshamariam, V.S. Vidhya, M. Jayachandran, Removal of Ni (II) ions on to polymer loaded sawdust (PLSD)-batch removal studies, *Fluid Mech.*, 3 (2016) 138–143.
- [25] A. Graillot, D. Bouyera, S. Monge, J.-J. Robin, C. Faura, Removal of nickel ions from aqueous solution by low energy-consuming sorption process involving thermosensitive copolymers with phosphonic acid groups, *J. Hazard. Mater.*, 244–245 (2013) 507–515.
- [26] A. Nezamzadeh-Ejhieh, M. Kabiri-Samani, Effective removal of Ni(II) from aqueous solutions by modification of nano particles of clinoptilolite with dimethylglyoxime, *J. Hazard. Mater.*, 260 (2013) 339–349.
- [27] M. Carmona, A. Pérez, A. de Lucas, L. Rodriguez, J.F. Rodriguez, Removal of chloride ions from an industrial polyethylenimine flocculant shifting it into an adhesive promoter using the anion exchange resin Amberlite IRA-420, *React. Funct. Polym.*, 68 (2008) 1218–1224.
- [28] R. Aravindhnan, N.N. Fathima, J.R. Rao, B.U. Nair, Equilibrium and Thermodynamic studies on the removal of basic black dye using calcium alginate beads, *Colloids Surf., A*, 299 (2007) 232–238.
- [29] H.N.M.E. Mahmud, S. Hosseini, R.B. Yahya, Removal of nickel ions from aqueous solution by polypyrrole conducting polymer, *Key Eng. Mater.*, 594–595 (2014) 793–797.
- [30] M. Borandegi, A. Nezamzadeh-Ejhieh, Enhanced removal efficiency of clinoptilolite nano-particles toward Co(II) from aqueous solution by modification with glutamic acid, *Colloids Surf., A*, 479 (2015) 35–45.
- [31] S. Langergren, B.K. Svenska, About the theory of so-called adsorption of soluble substances, *Zur theorie der sogenannten adsorption gel?ster stoffe*, K. Sven. Vetensk.akad. Handl., 24 (1898) 1–39.
- [32] Y.S. Ho, G. McKay, The kinetics of sorption of basic dyes from aqueous solutions by sphagnum moss peat, *Can. J. Chem. Eng.*, 76 (1998) 822–826.
- [33] M. Ozacar, I.A. Sengil, A kinetic study of metal complex dye sorption onto pine sawdust, *Process Biochem.*, 40 (2005) 565–572.
- [34] Y.S. Ho, G. McKay, Pseudo-second order model for sorption processes, *Process Biochem.*, 34 (1999) 451–465.
- [35] R.L. Tseng, Mesopore control of high surface area NaOH-activated carbon, *J. Colloid Interface Sci.*, 303 (2006) 494–502.
- [36] C. Namasivayam, M.V. Sureshkumar, Removal of chromium(VI) from water and wastewater using surfactant modified coconut coir pith as a biosorbent, *Bioresour. Technol.*, 99 (2008) 2218–2225.
- [37] F.W. Meng, Study on a Mathematical Model in Predicting Breakthrough Curves of Fixed-Bed Removal onto Resin Adsorbent, MS Thesis, Nanjing University, China, 2005, pp. 28–36.
- [38] G. McKay, M.S. Otterburn, J.A. Aja, Fuller's earth and fired clay as adsorbents for dye stuffs, *Water Air Soil Pollut.*, 24 (1985) 307–322.
- [39] W.J. Weber, J.C. Morris, J. Sanity, Kinetics of removal on carbon from solution, *J. Sanitary Eng. Div. Proc. Am. Soc. Civil Eng.*, 89 (1963) 31–59.
- [40] M. Sarkar, P.K. Acharya, B. Bhaskar, Modeling the removal kinetics of some priority organic pollutants in water from diffusion and activation energy parameters, *J. Colloid Interface Sci.*, 266 (2003) 28–32.

- [41] K. Kannan, M.M. Sundaram, Kinetics and mechanism of removal of methylene blue by removal on various carbons: a comparative study, *Dyes Pigment.*, 51 (2001) 25–40.
- [42] G.E. Boyd, A.W. Adamson, I.S. Myers, The exchange removal of ions from aqueous solutions by organic zeolites. II. Kinetics, *J. Am. Chem. Soc.*, 69 (1947) 2836–2848.
- [43] A.E. Ofomaja, Kinetic study and sorption mechanism of methylene blue and methyl violet onto mansonia (*Mansonia altissima*) wood sawdust, *Chem. Eng. J.*, 143 (2008) 85–95.
- [44] A. Naghash, A. Nezamzadeh-Ejehieh, Comparison of the efficiency of modified clinoptilolite with HDTMA and HDP surfactants for the removal of phosphate in aqueous solutions, *J. Ind. Eng. Chem.*, 31 (2015) 185–191.
- [45] F. Gode, E. Pehlivan, A comparative study of two chelating ion-exchange resins for the removal of chromium(III) from aqueous solution, *J. Hazard. Mater. B*, 100 (2003) 231–243.
- [46] G. Gode, E. Pehlivan, Removal of Cr(III) ions by Turkish brown coals, *Fuel Process. Technol.*, 86 (2005) 875–884.
- [47] Y.S. Ho, Effect of pH on lead removal from water using tree fern as the sorbent, *Bioresour. Technol.*, 96 (2005) 1292–1996.
- [48] M.M. Dubinin, E.D. Zaverina, L.V. Radushkevich, Sorption, and structure of activated carbons, I. Investigation of organic vapor removal, *Zh. Fiz. Khim.*, 21 (1947) 1351–1362.
- [49] N. Unlu, M. Ersoz, Removal characteristics of heavy metal ions onto a low-cost biopolymeric sorbents from aqueous solution, *J. Hazard. Mater.*, 136 (2006) 272–280.
- [50] A. Mohammad, A.K.R. Rifaqat, A. Rais, A. Jameel, Adsorption studies on *Citrus reticulata* (fruit peel of orange): removal and recovery of Ni(II) from electroplating wastewater, *J. Hazard. Mater.*, 79 (2000) 117–131.
- [51] Y.S. Ho, J.F. Porter, G. McKay, Equilibrium isotherm studies for the sorption of divalent metal ions onto peat: copper, nickel and lead single component systems, *Water Air Soil Pollut.*, 141 (2002) 1–33.
- [52] I.A.W. Tan, A.L. Ahmad, B.H. Hameed, Removal of basic dye using activated carbon prepared from oil palm shell: batch and fixed bed studies, *Desalination*, 225 (2008) 13–28.
- [53] A. Seker, T. Shahwan, A.E. Eroglu, Y. Sinan, Z. Demirel, M.C. Dalay, Equilibrium, thermodynamic and kinetic studies for the biosorption of aqueous lead(II), cadmium(II) and nickel(II) ions on *Spirulina platensis*, *J. Hazard. Mater.*, 154 (2008) 973–980.
- [54] F. Helfferich, *Ion Exchange*; McGraw-Hill, New York, 1962.
- [55] U.R. Malik, S.M. Hasany, M.S. Subhani, Sorptive potential of sunflower stem for Cr(III) ions from aqueous solutions and its kinetic and thermodynamic profile, *Talanta*, 66 (2005) 166–173.
- [56] J.M. Smith, *Chemical Engineering Kinetics*, McGraw-Hill, New York, 1981.
- [57] M. Anari-Anaraki, A. Nezamzadeh-Ejehieh, Modification of clinoptilolite nanoparticles by a cationic surfactant and dithizone for removal of Pb(II) from aqueous solution, *J. Colloid Interface Sci.*, 440 (2015) 272–281.
- [58] M. Heidari-Chaleshtoria, A. Nezamzadeh-Ejehieh, Modified clinoptilolite nano-particles with aspartic acid for removal of Cu(II) from aqueous solutions: isotherms and kinetic aspects, *New J. Chem.*, 39 (2015) 9396–9406.
- [59] B.H. Hameed, L.H. Chin, S. Rengaraj, Removal of 4-chlorophenol onto activated carbon prepared from rattan sawdust, *Desalination*, 225 (2008) 185–198.
- [60] M.I. Temkin, V. Pyzhev, Kinetics of ammonia synthesis on promoted iron catalysts, *Acta Physicochim*, 12 (1940) 327–356.
- [61] L.C. de Santa Maria, M.A.V. Souza, F.R. Santos, L.M.S. Rubenich, M.D.J.F. Ferreira, R.M.P. Sa, Thermogravimetric and spectrometric characterizations of poly(styrene-co-divinylbenzene) containing phosphinic and phosphonic acid groups, *Polym. Eng. Sci.*, 48 (2008) 1897–1900.